

Multiresolution Graph Transformers and Wavelet Positional Encoding for Learning Hierarchical Structures

Nhat Khang Ngo ^{*1} Truong Son Hy ^{*2} Risi Kondor ³

Abstract

Contemporary graph learning algorithms are not well-defined for large molecules since they do not consider the hierarchical interactions among the atoms, which are essential to determine the molecular properties of macromolecules. In this work, we propose Multiresolution Graph Transformers (MGT), the first graph transformer architecture that can learn to represent large molecules at multiple scales. MGT can learn to produce representations for the atoms and group them into meaningful functional groups or repeating units. We also introduce Wavelet Positional Encoding (WavePE), a new positional encoding method that can guarantee localization in both spectral and spatial domains. Our approach achieves competitive results on two macromolecule datasets consisting of polymers and peptides. Furthermore, the visualizations, including clustering results on macromolecules and low-dimensional spaces of their representations, demonstrate the capability of our methodology in learning to represent long-range and hierarchical structures.

1. Introduction

Macromolecules are long-range and hierarchical structures as they consist of many substructures. While small molecules in existing datasets (Ruddigkeit et al., 2012; Ramakrishnan et al., 2014; Sterling & Irwin, 2015) comprise less than 50 atoms connected by simple rings and bonds, this number in a macromolecule can be dozens or even hundreds. Substructures such as repeating units and functional groups are intrinsic parts of macromolecules; they present unique chemical reactions regardless of other compositions in the

same molecules (Jerry, 1992). Therefore, studying the multiresolution characteristic of large molecules is imperative to gain comprehensive knowledge about real-life materials like polymers or proteins (Schmid, 2022). In recent years, several works (Anand et al., 2022; Gaul & Cuesta-Lopez, 2022; Depta et al., 2022) have been proposed to apply machine learning algorithms to learn macromolecules at multiple scales. These approaches, however, rely on thorough feature selection and extraction, which are inefficient when learning from large databases of multicomponent materials (Anand et al., 2022).

Message passing is a prevailing paradigm for designing neural networks that operate on graph-structured data. Previous studies (Gilmer et al., 2017b; Kipf & Welling, 2016; Veličković et al., 2018; Corso et al., 2020b; Xu et al., 2019c) have proposed different strategies to perform message passing on graphs and achieved remarkable results across various domains. However, message-passing-dominated graph neural networks (GNNs) have some inherent limitations, such as limited expressiveness capability (Morris et al., 2019; Xu et al., 2019c), over-smoothing (Chen et al., 2020; Li et al., 2018; Oono & Suzuki, 2020), over-squashing (Alon & Yahav, 2021) issues. Over-smoothing exists in graph neural networks that consist of a sufficiently large number of layers, and node representations are likely to converge to a constant after going through these deep networks. Over-squashing problems occur when messages are ineffectively propagated and aggregated through bottlenecks on long-range graph structures. These two shortcomings hinder GNNs from making good predictions on long-range and hierarchically structured data. Furthermore, the molecular properties of large molecules are formed not only by interactions among atoms within neighborhoods but also by distant atoms. Therefore, local information is not sufficient to model macromolecules.

Transformers are classes of deep learning models that leverage self-attention mechanisms to handle long-range dependencies in various data domains, such as natural language processing (Vaswani et al., 2017; Devlin et al., 2019) or computer vision (Dosovitskiy et al., 2021; Liu et al., 2021). In graph domains, Transformer-like architectures (Kreuzer et al., 2021; Dwivedi & Bresson, 2020a; Rampášek et al.,

^{*}Equal contribution ¹FPT Software AI Center, Hanoi, Vietnam ²Halıcıoğlu Data Science Institute, University of California San Diego, La Jolla, USA ³Department of Computer Science, University of Chicago. Correspondence to: Truong Son Hy <tshy@ucsd.edu>.

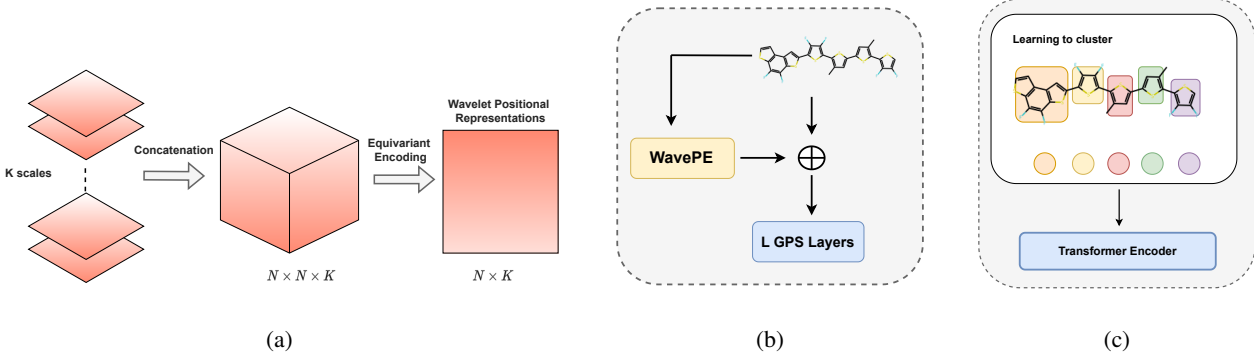


Figure 1. Overview of Wavelet Positional Encoding (WavePE) and Multiresolution Graph Transformer (MGT). a) k diffusion matrices of size $N \times N$ are stacked together to produce a wavelets tensor with size $N \times N \times K$ which are contracted by equivariant encoding methods to yield a tensor of positional representation $N \times k$. b) Atomic representations are derived by passing the molecular graph augmented with positional features through L GPS layers. c) A macromolecule is decomposed into several substructures in which the features are aggregated from the atom-level outputs, resulting in a set of substructures that are moved to a Transformer encoder.

2022) have proved their effectiveness in learning node representations as they can overcome the over-smoothing and over-squashing issues by directly measuring the pairwise relationships between the nodes. Contrary to GNNs, graph transformers do not use the graph structure as hard-coded information. They, instead, encode positional and structural information on graphs as soft inductive bias, making them flexible learners in graph learning problems (Kreuzer et al., 2021). Node positional representations can be derived based on spectral (Dwivedi & Bresson, 2020b; Dwivedi et al., 2022a) or spatial (You et al., 2019; Li et al., 2020b) domains. Most existing spectral-based methods decompose the graph Laplacian into sets of eigenvectors and eigenvalues. However, these eigenvectors have sign ambiguity and are unstable due to eigenvalue multiplicities. On the other hand, spatial-based approaches compute the shortest distances among the nodes; however, these encoding methods do not consider the structural similarity between nodes and their neighborhoods (Chen et al., 2022).

Contribution We propose Multiresolution Graph Transformer (MGT) and Wavelet Positional Encoding (WavePE), using multiresolution analysis on both spectral and spatial domains for learning to represent hierarchical structures. Our contributions are four-fold:

- We design Multiresolution Graph Transformer (MGT), a Transformer-like architecture that can operate on macromolecules at multiple scales. Our proposed model can learn the atomic representations and group them into meaningful clusters via a data-driven algorithm. Finally, the substructures, i.e. clusters, are fed to a Transformer encoder to calculate the representations of several substructures in macromolecules.

- We introduce Wavelet Positional Encoding (WavePE), a new positional encoding scheme for graph-structured data. Since wavelet analysis can provide localization in both spatial and spectral domains, we construct a set of wavelets to capture the structural information on graphs at different scales. Then, we apply equivariant encoding methods to project the wavelet tensors into positional representations for the atoms.
- We show the effectiveness of our methodology by reporting its superior performance on three molecular property prediction benchmarks. These datasets contain macromolecules, i.e. peptides and polymers, that are highly hierarchical and consist of up to hundreds of atoms.
- Our visualization demonstrates the comprehensiveness of our proposed methods in learning to represent large molecules. In general, we show the representations of molecules produced by MGT and how MGT determines and groups the atoms in long-chain molecules.

2. Related work

Hierarchical Learning on Molecule Functional groups or repeating units are essential phenomena in chemistry. While functional groups constitute large molecules, repeating units are the primary parts that produce complete polymer chains. We regard them as substructures. In particular, similar substructures undergo similar chemical reactions regardless of the remaining compositions existing in the molecules (Jerry, 1992). Previous work has leveraged the hierarchical property of molecules to improve the performance in molecular representation learning and generation. Fang et al. (2021), Rong et al. (2020), and Chen et al. (2021) used functional

groups as prior knowledge to guide the models to predict accurate molecular properties. For the molecular generation task, [Maziarz et al. \(2022\)](#) and [Jin et al. \(2020\)](#) used chemical rules to extract substructures and constructed a vocabulary of structural motifs to generate the molecules.

Graph Transformers Earlier research efforts have adopted Transformer-like architectures to graph-structured data. [Dwivedi & Bresson \(2020b\)](#) proposed an early approach to generalize Transformers to graphs using Laplacian positional encoding and performing self-attention on one-hop neighbors surrounding center nodes. On the other hand, [Kreuzer et al. \(2021\)](#) computes attention scores on the entire graph with differentiation between positive and negative edges, while also using Laplacian positional encoding. [Rong et al. \(2020\)](#) introduced GTransformer that utilizes vectorized outputs from local GNNs as inputs for a Transformer encoder, making up an effective combination between node local and global information. [Rampášek et al. \(2022\)](#) proposed a general framework that integrates essential components of Graph Transformers, including positional or structural encoding, graph feature extraction, local message passing, and self-attention. Also, [Chen et al. \(2022\)](#) extracted multiple k-hop subgraphs and fed them to local GNNs to compute their embeddings, which are then moved to a Transformer encoder. Graphomer proposed in [\(Ying et al., 2021\)](#) uses attention mechanisms to estimate several types of encoding, such as centrality, spatial, and edge encodings. In addition, [Kim et al. \(2022\)](#) treated all nodes and edges as independent tokens augmented with orthonormal node identifiers and trainable type identifiers, and fed them to a standard Transformer encoder. Moreover, [Yun et al. \(2019\)](#) generated multiple meta-paths, i.e. views, of a graph and computed their pairwise attention scores, before aggregating them into a final representation for the entire graph.

Graph Positional Encoding Several approaches have been proposed to encode the positional or structural representations into node features to improve the expressiveness of GNNs and Graph Transformers. Node positions can be determined via spectral or spatial domains. Spectral-based methods include Laplacian positional encoding ([Dwivedi & Bresson, 2020b](#); [Kreuzer et al., 2021](#)) and random walk positional encoding (RWPE) ([Dwivedi et al., 2022a](#)). For spatial-based methods, [You et al. \(2019\)](#) computed distances of sets of nodes to anchor nodes, whereas [Li et al. \(2020b\)](#) calculated the shortest distances between pairs of nodes.

Multiresolution Analysis and Wavelet Theory Multiresolution Analysis (MRA) has been proposed by ([Mallat, 1989; 2008](#)) as a method to approximate signals at multiple scales in which the signals are decomposed over elementary waveforms chosen from a family called wavelets (i.e.

mother wavelets and father wavelets), including Haar ([Haar, 1910](#)), Daubechies ([Daubechies, 1988](#)), etc., to produce the sparse representations. In graph and discrete domains, [Hammond et al. \(2011\)](#) introduced spectral graph wavelets that are determined by applying the wavelet operator on the graph Laplacian at multi-levels. [Coifman & Maggioni \(2006\)](#) proposed diffusion wavelet that is a fast multiresolution framework for analyzing functions on discretized structures such as graphs and manifolds. In the deep learning era, [Rustamov & Guibas \(2013\)](#) and [Xu et al. \(2019b\)](#) leveraged the power of neural networks for graph wavelet construction and computation.

3. Preliminaries

3.1. Notation

A molecule can be represented as an undirected graph in which nodes are the atoms and edges are the bonds between them. In particular, we refer to a molecular graph as $G = (\mathcal{V}, \mathcal{E}, \mathbf{A}, \mathbf{X}, \mathbf{P}, \mathcal{V}_s)$, where G is an undirected graph having $\mathcal{V} (|\mathcal{V}| = n)$ and \mathcal{E} as sets of nodes and edges respectively; also, $\mathbf{A} \in \mathbb{R}^{n \times n}$ is the graph's adjacency matrix. When a graph is attributed, we augment G with a set of node feature vectors $\mathcal{X} = \{x_1, \dots, x_n\}, x_i \in \mathbb{R}^d$ and a set of node positional vectors $\mathcal{P} = \{p_1, \dots, p_n\}, p_i \in \mathbb{R}^p$. These two types of attributes are stored in $\mathbf{X} \in \mathbb{R}^{n \times d}$ and $\mathbf{P} \in \mathbb{R}^{n \times p}$ correspondingly. In addition to the atom-level representation of G , $\mathcal{V}_s = \{v_{s_1}, \dots, v_{s_k}\}$ denotes the substructure set in which $v_{s_i} \subset \mathcal{V}$, i.e. v_{s_i} is a subset of atoms of the molecule.

3.2. Hierarchical Learning on Molecules

Molecular property prediction is regarded as a graph-level learning task. We need to aggregate node embeddings into graph-level vectors which are then fed to a classifier to make predictions on graphs. Specifically, a function $f : \mathcal{V} \rightarrow \mathcal{Z}$ that maps the atom $u \in \mathcal{V}$ to a d_o -dimensional vector $z_u \in \mathcal{Z} \subset \mathbb{R}^{d_o}$ should learn to produce atom-level representations. Most existing graph neural networks compute the vector $z = \zeta(\{f(u) | u \in \mathcal{V}\})$ that indicates a representation for the entire molecular graph, where ζ can be sum, mean, max, or more sophisticated operators. For hierarchical learning, substructure-level representations can be derived in addition to atom-level representations by aggregating node representations in the same substructures as $z_s = \zeta(\{f(u) | u \in v_s \wedge v_s \in \mathcal{V}_s\})$. Instead of atom vectors, we aggregate the substructure vectors to represent the entire graph, i.e. $z = \zeta(\{z_s | z_s \in \mathcal{V}_s\})$. Finally, a classifier g given z as inputs is trained to predict the molecular properties.

3.3. Transformers on Graphs

While GNNs learn node embeddings by leveraging the graph structure via local message-passing mechanisms, Transformers ignore localities and directly infer the relations between pairs of nodes using only node attributes. In other words, the node connectivity is not utilized in pure transformer-like architectures (Vaswani et al., 2017), reducing the graph conditions to a set learning problem. Given a tensor of node features $\mathbf{X} \in \mathbb{R}^{n \times d}$, Transformers compute three matrices including query (\mathbf{Q}), key (\mathbf{K}), and value (\mathbf{V}) via three linear transformations $\mathbf{Q} = \mathbf{X}\mathbf{W}_q^T$, $\mathbf{K} = \mathbf{X}\mathbf{W}_k^T$, and $\mathbf{V} = \mathbf{X}\mathbf{W}_v^T$. A self-attention tensor (\mathbf{H}) can be computed as follows:

$$\mathbf{H} = \text{softmax}\left(\frac{\mathbf{Q}\mathbf{K}^T}{\sqrt{d_o}}\right)\mathbf{V} \quad (1)$$

where \mathbf{W}_q , \mathbf{W}_k , and \mathbf{W}_v are learnable parameters in $\mathbb{R}^{d_o \times d}$, resulting in $\mathbf{H} \in \mathbb{R}^{n \times d_o}$. Furthermore, each \mathbf{H} in Eq. 1 denotes an attention head. To improve effectiveness, multiple $\{\mathbf{H}_i\}_{i=1}^h$ are computed, which is known as multi-head attention. All of the attention heads are concatenated to form a final tensor: $\mathbf{H}_o = \text{concat}(\mathbf{H}_1, \dots, \mathbf{H}_h)$, where h is the number of attention heads. Finally, the output \mathbf{X}' , i.e. new node representations, can be computed by feeding \mathbf{H}_o into a feed-forward neural network (FFN), i.e. $\mathbf{X}' = \text{FFN}(\mathbf{H}_o)$. It is easy to see that Transformers operating on inputs without positional encoding are permutation invariant.

Positional Encoding As pure Transformer encoders only model sets of nodes without being cognizant of the graph structures, positional or structural information between nodes and their neighborhoods should be incorporated into node features. In particular, node positional representations can be added or concatenated with node features, resulting in comprehensive inputs for Transformer-like architectures operating on graph-structured data.

4. Wavelet Positional Encoding

4.1. Spectral Graph Wavelets

Let $\mathcal{A} \in \mathbb{R}^{n \times n}$ be the adjacency matrix of an undirected graph $G = (\mathcal{V}, \mathcal{E})$. The normalized graph Laplacian is defined as $\mathcal{L} = \mathcal{I}_n - \mathcal{D}^{-1/2} \mathcal{A} \mathcal{D}^{-1/2}$, where \mathcal{I}_n is the identity matrix and \mathcal{D} is the diagonal matrix of node degrees. \mathcal{L} can be decomposed into a complete set of orthonormal eigenvectors $U = (u_1, u_2, \dots, u_n)$ associated with real and non-negative eigenvalues $\{\lambda\}_1^n$. While graph Fourier transform uses U as a set of bases to project the graph signal from the vertex domain to the spectral domain, graph wavelet transform constructs a set of spectral graph wavelets as bases for this projection via:

$$\psi_s = U \Sigma_s U^T$$

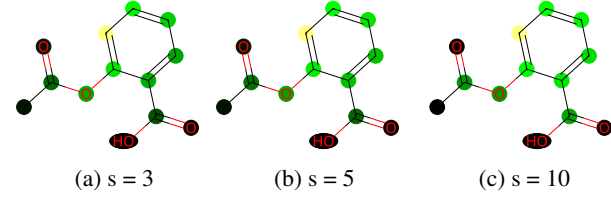


Figure 2. Visualization of some of the wavelets with scaling parameters on the Aspirin $C_9H_8O_4$ molecular graph with 13 nodes (i.e. heavy atoms). The center node is colored yellow. The colors varying from bright to dark illustrate the diffusion rate from the center node to the others, i.e. nodes that are closer to the center node have brighter colors. Low-scale wavelets are highly localized, whereas the high-scale wavelets can spread out more nodes on the molecular graphs

where $\Sigma_s = \text{diag}(g(s\lambda_1), g(s\lambda_2), \dots, g(s\lambda_n))$ is a scaling matrix of eigenvalues, $\psi_s = (\psi_{s1}, \psi_{s2}, \dots, \psi_{sn})$ and each wavelet ψ_{si} indicates how a signal diffuses away from node i at scale s ; we choose $g(s\lambda) = e^{-s\lambda}$ as a heat kernel (Donnat et al., 2018). Since a node's neighborhoods can be adjusted by varying the scaling parameter s (Xu et al., 2019a), using multiple sets of wavelets at different scales can provide comprehensive information on the graph's structure. It means that larger values of s_i correspond to larger neighborhoods surrounding a center node. Figure 2 illustrates how wavelets can be used to determine neighborhoods at different scales on a molecular graph. In this work, we leverage this property of graph wavelets to generate node positional representations that can capture the structural information of a center node on the graph at different resolutions. We employ k diffusion matrices $\{\psi_{si}\}_{i=1}^k$ in which each ψ_{si} has a size of $n \times n$, resulting in a tensor of graph wavelets $\mathcal{P} \in \mathbb{R}^{n \times n \times k}$. Additionally, WavePE is a generalized version of RWPE (Dwivedi et al., 2022a) as the random walk process can be regarded as a type of discrete diffusion. In the following section, we demonstrate the use of tensor contractions to generate a tensor of node positional representations $\mathbf{P} \in \mathbb{R}^{n \times k}$ from \mathcal{P} . In general, Fig.1a demonstrates our wavelet positional encoding method.

4.2. Equivariant Encoding

It is important to note that our spectral graph wavelets computed from the previous section must be further encoded in a permutation-equivariant manner. For simplicity, that means if we permute (i.e. change the order) the set of nodes, their position encodings must be transformed accordingly. In this section, we formally define permutation symmetry, i.e. symmetry to the action of the symmetric group, \mathbb{S}_n , and construct permutation-equivariant neural networks to encode graph wavelets. An element $\sigma \in \mathbb{S}_n$ is a permutation of order n , or a bijective map from $\{1, \dots, n\}$ to

$\{1, \dots, n\}$. For example, the action of \mathbb{S}_n on an adjacency matrix $\mathcal{A} \in \mathbb{R}^{n \times n}$ and on a latent matrix $\mathcal{Z} \in \mathbb{R}^{n \times d_z}$ are:

$$[\sigma \cdot \mathcal{A}]_{i_1, i_2} = \mathcal{A}_{\sigma^{-1}(i_1), \sigma^{-1}(i_2)}, \quad [\sigma \cdot \mathcal{Z}]_{i, j} = \mathcal{Z}_{\sigma^{-1}(i), j},$$

for $\sigma \in \mathbb{S}_n$. Here, the adjacency matrix \mathcal{A} is a second-order tensor with a single feature channel, while the latent matrix \mathcal{Z} is a first-order tensor with d_z feature channels. In general, the action of \mathbb{S}_n on a k -th order tensor $\mathcal{X} \in \mathbb{R}^{n^k \times d}$ (i.e. the last index denotes the feature channels) is defined similarly as:

$$[\sigma \cdot \mathcal{X}]_{i_1, \dots, i_k, j} = \mathcal{X}_{\sigma^{-1}(i_1), \dots, \sigma^{-1}(i_k), j}, \quad \sigma \in \mathbb{S}_n.$$

Formally, we define these equivariant and invariant properties in Def. 4.1 and equivariant neural networks in Def. 4.2.

Definition 4.1. An \mathbb{S}_n -equivariant (or permutation equivariant) function is a function $f: \mathbb{R}^{n^k \times d} \rightarrow \mathbb{R}^{n^{k'} \times d'}$ that satisfies $f(\sigma \cdot \mathcal{X}) = \sigma \cdot f(\mathcal{X})$ for all $\sigma \in \mathbb{S}_n$ and $\mathcal{X} \in \mathbb{R}^{n^k \times d}$. Similarly, we say that f is \mathbb{S}_n -invariant (or permutation invariant) if and only if $f(\sigma \cdot \mathcal{X}) = f(\mathcal{X})$.

Definition 4.2. An \mathbb{S}_n -equivariant network is a function $f: \mathbb{R}^{n^k \times d} \rightarrow \mathbb{R}^{n^{k'} \times d'}$ defined as a composition of \mathbb{S}_n -equivariant linear functions f_1, \dots, f_T and \mathbb{S}_n -equivariant nonlinearities $\gamma_1, \dots, \gamma_T$:

$$f = \gamma_T \circ f_T \circ \dots \circ \gamma_1 \circ f_1.$$

On the another hand, an \mathbb{S}_n -invariant network is a function $f: \mathbb{R}^{n^k \times d} \rightarrow \mathbb{R}$ defined as a composition of an \mathbb{S}_n -equivariant network f' and an \mathbb{S}_n -invariant function on top of it, e.g., $f = f'' \circ f'$.

In order to build permutation-equivariant neural networks, we revisit some basic tensor operations: the tensor product $A \otimes B$ (see Def. 4.3) and tensor contraction $A \downarrow_{x_1, \dots, x_p}$ (see Def. 4.4). It can be shown that these tensor operations respect permutation equivariance (Hy et al., 2018) (Kondor et al., 2018).

Definition 4.3. The **tensor product** of $A \in \mathbb{R}^{n^a}$ with $B \in \mathbb{R}^{n^b}$ yields a tensor $C = A \otimes B \in \mathbb{R}^{n^{a+b}}$ where

$$C_{i_1, i_2, \dots, i_{a+b}} = A_{i_1, i_2, \dots, i_a} B_{i_{a+1}, i_{a+2}, \dots, i_{a+b}}.$$

Definition 4.4. The **contraction** of $A \in \mathbb{R}^{n^a}$ along the pair of dimensions $\{x, y\}$ (assuming $x < y$) yields a $(a-2)$ -th order tensor

$$C_{i_1, \dots, i_{x-1}, j, i_{x+1}, \dots, i_{y-1}, j, i_{y+1}, \dots, i_a} = \sum_{i_x, i_y} A_{i_1, \dots, i_a},$$

where we assume that i_x and i_y have been removed from amongst the indices of C . Using Einstein notation, this can be written more compactly as

$$C_{\{i_1, i_2, \dots, i_a\} \setminus \{i_x, i_y\}} = A_{i_1, i_2, \dots, i_a} \delta^{i_x, i_y},$$

where δ is the Kronecker delta. In general, the contraction of A along dimensions $\{x_1, \dots, x_p\}$ yields a tensor $C = A \downarrow_{x_1, \dots, x_p} \in \mathbb{R}^{n^{a-p}}$ where

$$A \downarrow_{x_1, \dots, x_p} = \sum_{i_{x_1}} \sum_{i_{x_2}} \dots \sum_{i_{x_p}} A_{i_1, i_2, \dots, i_a},$$

or compactly as

$$A \downarrow_{x_1, \dots, x_p} = A_{i_1, i_2, \dots, i_a} \delta^{i_{x_1}, i_{x_2}, \dots, i_{x_p}}.$$

Based on these tensor contractions and Def. 4.1, we can construct the second-order \mathbb{S}_n -equivariant networks encoding a graph with adjacency matrix $\mathcal{A} \in \mathbb{R}^{n \times n}$, node features $\mathcal{F}_v \in \mathbb{R}^{n \times d_v}$ and edge features $\mathbb{R}^{n \times n \times d_e}$ as in Section 4.2.1:

$$f = \gamma \circ \mathcal{M}_T \circ \dots \circ \gamma \circ \mathcal{M}_1.$$

The “raw” graph wavelets can be treated as a second-order tensor of size $n \times n \times k$ where k is the number of scales, similarly as the edge features. We employ the higher-order permutation-equivariant message passing proposed by (Maron et al., 2019), (Hy et al., 2018) and (Kondor et al., 2018) to encode the “raw” graph wavelets from size $n \times n \times k$ into $n \times k$ that will be further used as nodes/tokens’ embeddings of our Transformer architecture (see Fig. 1).

4.2.1. HIGHER-ORDER MESSAGE PASSING

The second order message passing has the message $\mathcal{H}_0 \in \mathbb{R}^{|\mathcal{V}| \times |\mathcal{V}| \times (d_v + d_e)}$ initialized by promoting the node features \mathcal{F}_v to a second order tensor (e.g., we treat node features as self-loop edge features), and concatenating with the edge features \mathcal{F}_e . Iteratively,

$$\mathcal{H}_t = \gamma(\mathcal{M}_t), \quad \mathcal{M}_t = \mathcal{W}_t \left[\bigoplus_{i,j} (\mathcal{A} \otimes \mathcal{H}_{t-1}) \downarrow_{i,j} \right],$$

where $\mathcal{A} \otimes \mathcal{H}_{t-1}$ results in a fourth order tensor while $\downarrow_{i,j}$ contracts it down to a second order tensor along the i -th and j -th dimensions, \oplus denotes concatenation along the feature channels, and \mathcal{W}_t denotes a multilayer perceptron on the feature channels. We remark that the popular MPNNs (Gilmer et al., 2017a) is a lower-order one and a special case in which $\mathcal{M}_t = \mathcal{D}^{-1} \mathcal{A} \mathcal{H}_{t-1} \mathcal{W}_{t-1}$ where $\mathcal{D}_{ii} = \sum_j \mathcal{A}_{ij}$ is the diagonal matrix of node degrees. The message \mathcal{H}_T of the last iteration is still second order, so we contract it down to the first order latent $\mathcal{Z} = \bigoplus_i \mathcal{H}_{T \downarrow i}$.

5. Multiresolution Graph Transformers

In this section, we present Multiresolution Graph Transformers (MGT), a neural network architecture for learning hierarchical structures. MGT uses Transformers to yield the representations of macromolecules at different resolutions. While previous work either neglects the hierarchical

characteristics of large molecules or fails to model global interactions between distant atoms, our proposed approach can satisfy these two properties via multiresolution analysis.

Figs. 1b and 1c show an overview of our framework. MGT consists of three main components: an atom-level encoder, a module to extract substructures, and a substructure-level encoder. We use a graph transformer to generate the atomic embeddings. Then, substructures present in molecules are extracted by a learning-to-cluster algorithm. The molecular graph is coarsened into a set of substructures, and we use a pure Transformer encoder to learn their relations.

5.1. Atom-Level Encoder

To utilize the proposed wavelet positional encoding demonstrated in Section 4, we leverage the design of the graph transformer proposed in (Rampášek et al., 2022), which is a general, powerful, and scalable Graph Transformer (GraphGPS) for graph representation learning. Let $\mathbf{A} \in \mathbb{R}^{n \times n}$ be the adjacency matrix of a graph with n nodes and e edges; \mathbf{X}^l and \mathbf{E}^l are node and edge features at layer l -th, respectively. In addition, $\mathbf{X}^0 \in \mathbb{R}^{n \times d}$ and $\mathbf{E}^0 \in \mathbb{R}^{e \times d}$ are initial atom and bond features embedded in d -dimensional spaces created by two embedding layers. The wavelet positional vectors $\mathbf{p} \in \mathbb{R}^{n \times k}$ are fed to an encoder (e.g., a feed-forward neural network or a linear transformation), yielding a tensor of positional features $\mathbf{P} \in \mathbb{R}^{n \times d_p}$. We let $\mathbf{X}^0 := \text{concat}(\mathbf{X}^0, \mathbf{P})$ to produce new node features $\mathbf{X}^0 \in \mathbb{R}^{n \times (d+d_p)}$. From here, we define $d := d + d_p$, and for convenience, the output dimensions of all layers are equal to d .

Each layer of GraphGPS uses a message-passing neural network (MPNN^l) to exchange information (i.e., messages) within the neighborhood and a self-attention layer (SA^l) described in Eq. (1) to compute global interactions among distant nodes:

$$\mathbf{X}_L^{l+1}, \mathbf{E}^{l+1} = \text{MPNN}^l(\mathbf{X}^l, \mathbf{E}^l, \mathbf{A}) \quad (2)$$

$$\mathbf{X}_G^{l+1} = \text{SA}^l(\mathbf{X}^l) \quad (3)$$

$$\mathbf{X}^{l+1} = \text{FFN}^l(\mathbf{X}_L^{l+1} + \mathbf{X}_G^{l+1}) \quad (4)$$

where \mathbf{X}_L^{l+1} and \mathbf{X}_G^{l+1} are node local and global representations; they are unified into \mathbf{X}^{l+1} via Eq. 4. Popular techniques such as Dropout (Srivastava et al., 2014) and normalization (Ioffe & Szegedy, 2015; Ba et al., 2016) are omitted for the sake of clarity. By feeding the molecular graph through L layers, we attain two tensors $\mathbf{X}_a := \mathbf{X}^L$ and $\mathbf{E}_a := \mathbf{E}^L$ indicating the node and edge embeddings, respectively.

5.2. Learning to Cluster

In this work, we use a message-passing neural network augmented with differentiable pooling layers (Ying et al.,

2018) to cluster the atoms into substructures automatically:

$$\mathbf{Z} = \text{MPNN}_e(\mathbf{X}_a, \mathbf{E}_a, \mathbf{A}) \quad (5)$$

$$\mathbf{S} = \text{Softmax}(\text{MPNN}_c(\mathbf{X}_a, \mathbf{E}_a, \mathbf{A})) \quad (6)$$

where MPNN_e and MPNN_c are two-layer message-passing networks that learn to generate node embeddings ($\mathbf{Z} \in \mathbb{R}^{n \times d}$) and a clustering matrix ($\mathbf{S} \in \mathbb{R}^{n \times C}$), respectively; C denotes the number of substructures in molecules. A tensor of features $\mathbf{X}_s \in \mathbb{R}^{C \times d}$ for the substructures is computed:

$$\mathbf{X}_s = \mathbf{S}^T \mathbf{Z} \quad (7)$$

This learning-to-cluster module is placed after the atom-level encoder. Intuitively, atom nodes updated with both local and global information should be classified into accurate substructures.

5.3. Substructure-level Encoder

Given a set of substructures \mathcal{V}_s with a tensor of features $\mathbf{X}_s \in \mathbb{R}^{C \times d}$, we forward \mathbf{X}_s to L conventional Transformer encoder layers (Vaswani et al., 2017) to capture their pairwise semantics:

$$\mathbf{H}_1^{l+1} = \text{Norm}(\text{SA}^l(\mathbf{H}^l) + \mathbf{H}^l) \quad (8)$$

$$\mathbf{H}_1^{l+1} = \text{Norm}(\text{FFN}(\mathbf{H}_1^{l+1}) + \mathbf{H}_1^{l+1}) \quad (9)$$

where SA refers to (multi-head) self-attention described in Eq. (1), and \mathbf{H}^0 is equal to \mathbf{X}_s . Additionally, we add a long-range skip connection to alleviate gradient vanishing as:

$$\mathbf{H}_s = \text{FFN}(\text{concat}(\mathbf{H}^0, \mathbf{H}^L)) \quad (10)$$

$\mathbf{H}_s \in \mathbb{R}^{C \times d}$ is the output indicating the representations for the substructures. Finally, we aggregate all C vectors $h_s \in \mathbf{H}_s$ to result in a unique representation $z \in \mathbb{R}^d$ for the molecules (refer to Section 3.2), before feeding it to a feed-forward network to compute the final output $y \in \mathbb{R}^c$ for property prediction:

$$z = \zeta(\{h_s\}_{s=1}^C) \quad (11)$$

$$\hat{y} = \text{FFN}(z) \quad (12)$$

Training Objective We train MGT by minimizing \mathcal{L} :

$$\mathcal{L} = \mathcal{L}_1 + \lambda_1 \mathcal{L}_{LP} + \lambda_2 \mathcal{L}_E \quad (13)$$

where $\mathcal{L}_1 = l(\hat{y}, y)$ denotes the loss function between predicted values and ground truths (e.g., cross-entropy or mean-squared error), $\mathcal{L}_{LP} = \|\mathbf{A} - \mathbf{S}^T \mathbf{S}\|_F$ indicates auxiliary link prediction loss ($\|\cdot\|_F$ denotes the Frobenius norm), and $\mathcal{L}_E = \frac{1}{n} \sum_{i=1}^n H(\mathbf{S}_i)$ denotes the entropy regularization of the cluster assignment, i.e. each atom should be assigned into a unique cluster. Additionally, λ_1 and λ_2 are hyperparameters.

Table 1. Results on peptides property prediction

Model	No.Params	Peptides-struct	Peptides-func
		MAE ↓	AP ↑
GCN	508k	0.3496 ± 0.0013	0.5930 ± 0.0023
GINE	476k	0.3547 ± 0.0045	0.5498 ± 0.0079
GatedGCN	509k	0.3420 ± 0.0013	0.5864 ± 0.0077
GatedGCN + RWPE	506k	0.3357 ± 0.0006	0.6069 ± 0.0035
Transformer + LapPE	488k	0.2529 ± 0.0016	0.6326 ± 0.0126
SAN + LapPE	493k	0.2683 ± 0.0043	0.6384 ± 0.0121
SAN + RWPE	500k	0.2545 ± 0.0012	0.6562 ± 0.0075
MGT + LapPE (ours)	499k	0.2488 ± 0.0014	0.6728 ± 0.0152
MGT + RWPE (ours)	499k	0.2496 ± 0.0009	0.6709 ± 0.0083
MGT + WavePE (ours)	499k	0.2453 ± 0.0025	0.6817 ± 0.0064

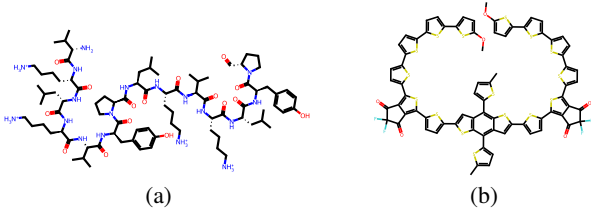


Figure 3. Examples of two macromolecules. a) An example of a peptide that consists of many functional groups. b) An example of a polymer that consists of many repeating units

6. Experiments

We empirically validate our proposed approach in two types of macromolecules including peptides and polymers. Figure 3 illustrates two examples of macromolecules in the datasets.

6.1. Peptides Property Prediction

Peptides are small chains of amino acids found in nature that serve a variety of critical biological roles (Singh et al., 2016); however, they are far shorter than proteins. Because each amino acid is made up of several heavy atoms, a peptide’s molecular graph is significantly greater than that of a tiny drug-like molecule. Since peptides are formed by sequences of amino acids, they are naturally hierarchical and long-range dependencies (Dwivedi et al., 2022b), i.e. a peptide should be ideally segmented into an exact set of amino acids. Therefore, we evaluate our method on peptide structures to demonstrate its superiority.

Experimental Setup We run experiments on two real-world datasets including (1) Peptides-struct and (2) Peptides-func (Dwivedi et al., 2022b). The two datasets are multi-

label graph classification problems and share the same peptide molecular graphs, but with different tasks. While the former consists of 10 classes based on peptides function, the latter is used to predict 11 aggregated 3D properties of peptides at the graph level. For a fair comparison, we follow the experimental and evaluation setting of (Dwivedi et al., 2022b) with the same train/test split ratio. We use mean absolute error (MAE) and average precision (AP) to evaluate the method’s performance for Peptides-struct and Peptides-func, respectively.

Baselines and Implementation Details We compare our proposed approach with the baselines taken from (Dwivedi et al., 2022b). The local message-passing network class involves GCN (Kipf & Welling, 2016), GCNII (Bresson & Laurent, 2017), GINE (Xu et al., 2019c; Hu et al., 2020), and GatedGCN (Bresson & Laurent, 2017). For Transformer-based architectures, we compare our method with vanilla Transformer (Vaswani et al., 2017) with Laplacian PE (Dwivedi et al., 2020; Dwivedi & Bresson, 2020b) and SAN (Kreuzer et al., 2021). Since all baselines are limited to approximately 500k learnable parameters, we also restrict MGT to roughly the same number of parameters. Additionally, we use GatedGCN (Bresson & Laurent, 2017) for local message passing customized with the PEG technique to stabilize the positional features (Wang et al., 2022)¹. We experiment with each task in four different random seeds. We provide further implementation details of MGT for this task in Appendix A.1.

Results Table 1 shows that our proposed MGT + WavePE achieves the best performances in two peptide prediction tasks. In addition to WavePE, MGT + RWPE also attains

¹The implementation of GPS is adapted from <https://github.com/vijaydwivedi75/lrgb.git>.

the second-best performances. The superiority of WavePE to RWPE can be explained as mentioned in Section 4 that WavePE is a generalized version of RWPE. In particular, our proposed MGT outperforms all the baselines in the Petides-func task by a large margin and decreases the MAE score to less than 0.25 in the Petides-struct task.

6.2. Polymer Property Prediction

Polymers are long chains of repetitive substructures known as repeating units. They, as a result, are also hierarchically structured and contain various types of long-range dependencies among the atoms. Since polymers have a wide range of applications in daily life, it is essential to understand their molecular properties. In this work, we experiment on a dataset of polymers to verify the superior performance of MGT in predicting molecular properties, as well as detecting repeating units existing in polymer structures.

Experimental Setup We use a polymer dataset proposed in (St. John et al., 2019). Each polymer is associated with three types of Density Functional Theory (DFT) (Hohenberg & Kohn, 1964) properties including the first excitation energy of the monomer calculated with time-dependent DFT (GAP), the energy of the highest occupied molecular orbital for the monomer (HOMO), and the lowest unoccupied molecular orbital of the monomer (LUMO). The dataset is split into train/validation/test subsets with a ratio of 8:1:1, respectively. For training, we normalize all learning targets to have a mean of 0 and a standard deviation of 1.

Baselines and Implementation Details As there are no existing baselines on this dataset, we perform experiments with four different models for comparisons. For local GNNs, we use GCN (Kipf & Welling, 2016) and GINE (Xu et al., 2019c; Hu et al., 2020) augmented with virtual nodes as the baselines². Moreover, we use standard Transformer (Vaswani et al., 2017) with Laplacian positional encoding (Dwivedi & Bresson, 2020b) and GPS (Rampášek et al., 2022) as the baselines for Transformer-based architectures. The implementation of MGT is similar to the Peptide tasks. Please refer to Appendix A.2 for the baseline details.

Results As shown in Table 2, our MGT models achieve the lowest MAE scores across three properties. In addition, WavePE can attain comparable results with LapPE and RWPE for this task. We observe that the vanilla Transformer has the poorest performance. This demonstrates that computing global information without the awareness of locality is not sufficient for macromolecular modeling. As described in Section 5, MGT is an extended version of GPS. In particular, a learning-to-cluster module and a

²The implementation of local GNN models is taken from <https://github.com/snap-stanford/ogb/tree/master/ogb>

substructure-level Transformer encoder are extensions to GPS. The better performance of MGT, as a result, indicates that our methodology in modeling hierarchical structures is appropriate and reasonable.

6.3. Visualization

In addition to numerical results, we provide some visualizations to demonstrate the comprehensiveness of MGT in learning to represent large molecules. For visual quality purposes, we place the figures in the Appendix. Figs. 4 and 5 show clear and smooth clustering patterns in low-dimensional spaces that indicate our proposed approaches are able to learn meaningful molecular representations for hierarchical structures such as peptides and polymers. Furthermore, according to Figs. 6 and 7, our learning-to-cluster algorithm and multiresolution analysis can pick up functional groups (for proteins/peptides) and repeating units (for polymers) via back-propagation.

7. Conclusion

In this work, we introduce the MGT model and WavePE method, which perform multiresolution analysis in both spatial and spectral domains. Our proposed methods can learn to represent hierarchical and long-range structures. In addition to numerical performance, MGT can provide interpretable clustering results and produce discernible spaces of the representations of large molecules.

References

- Alon, U. and Yahav, E. On the bottleneck of graph neural networks and its practical implications. In *International Conference on Learning Representations*, 2021. URL <https://openreview.net/forum?id=i800OPhOCVH2>.
- Anand, G., Ghosh, S., Zhang, L., Anupam, A., Freeman, C. L., Ortner, C., Eisenbach, M., and Kermode, J. R. Exploiting machine learning in multiscale modelling of materials. *Journal of The Institution of Engineers (India): Series D*, Nov 2022. ISSN 2250-2130. doi: 10.1007/s40033-022-00424-z. URL <https://doi.org/10.1007/s40033-022-00424-z>.
- Ba, L. J., Kiros, J. R., and Hinton, G. E. Layer normalization. *CoRR*, abs/1607.06450, 2016. URL <http://arxiv.org/abs/1607.06450>.
- Bresson, X. and Laurent, T. Residual gated graph convnets. *CoRR*, abs/1711.07553, 2017. URL <http://arxiv.org/abs/1711.07553>.
- Chen, D., Lin, Y., Li, W., Li, P., Zhou, J., and Sun, X. Measuring and relieving the over-smoothing problem

Table 2. Experimental results on the polymer property prediction task. All the methods are trained in four different random seeds and evaluated by MAE ↓. Our methods are able to attain better performance across three DFT properties of polymers while having less number of parameters. All the properties are measured in eV.

Model	No. Params	Property		
		GAP	HOMO	LUMO
GCN + Virtual Node	557k	0.1130 ± 0.0009	0.0100 ± 0.0016	0.0871 ± 0.0019
GINE + Virtual Node	557k	0.1669 ± 0.0078	0.1233 ± 0.0130	0.0945 ± 0.0028
GPS	600k	0.0895 ± 0.0032	0.0703 ± 0.0045	0.0695 ± 0.0011
Transformer + LapPE	700k	0.5653 ± 0.0923	0.2621 ± 0.0450	0.2791 ± 0.0229
MGT + LapPE (ours)	499k	0.0724 ± 0.0008	0.0590 ± 0.0025	0.0533 ± 0.0006
MGT + RWPE (ours)	499k	0.0736 ± 0.0031	0.0600 ± 0.0011	0.0523 ± 0.0015
MGT + WavePE (ours)	499k	0.0741 ± 0.0023	0.0619 ± 0.0009	0.0539 ± 0.0020

for graph neural networks from the topological view. *Proceedings of the AAAI Conference on Artificial Intelligence*, 34(04):3438–3445, Apr. 2020. doi: 10.1609/aaai.v34i04.5747. URL <https://ojs.aaai.org/index.php/AAAI/article/view/5747>.

Chen, D., O’Bray, L., and Borgwardt, K. Structure-aware transformer for graph representation learning. In *Proceedings of the 39th International Conference on Machine Learning (ICML)*, Proceedings of Machine Learning Research, 2022.

Chen, F., Park, J., and Park, J. A hypergraph convolutional neural network for molecular properties prediction using functional group. *CoRR*, abs/2106.01028, 2021. URL <https://arxiv.org/abs/2106.01028>.

Coifman, R. R. and Maggioni, M. Diffusion wavelets. *Applied and Computational Harmonic Analysis*, 21(1):53–94, 2006. ISSN 1063-5203. doi: <https://doi.org/10.1016/j.acha.2006.04.004>. URL <https://www.sciencedirect.com/science/article/pii/S106352030600056X>. Special Issue: Diffusion Maps and Wavelets.

Corso, G., Cavalleri, L., Beaini, D., Liò, P., and Velickovic, P. Principal neighbourhood aggregation for graph nets. In *Proceedings of the 34th International Conference on Neural Information Processing Systems*, NIPS’20, Red Hook, NY, USA, 2020a. Curran Associates Inc. ISBN 9781713829546.

Corso, G., Cavalleri, L., Beaini, D., Liò, P., and Veličković, P. Principal neighbourhood aggregation for graph nets. In Larochelle, H., Ranzato, M., Hadsell, R., Balcan, M., and Lin, H. (eds.), *Advances in Neural Information Processing Systems*, volume 33, pp. 13260–13271. Curran Associates, Inc., 2020b. URL <https://proceedings.neurips.cc/paper/2020/file>

[99cad265a1768cc2dd013f0e740300ae-Paper.pdf](https://www.semanticscience.org/99cad265a1768cc2dd013f0e740300ae-Paper.pdf).

Daubechies, I. Orthonormal bases of compactly supported wavelets. *Communications on Pure and Applied Mathematics*, 41:909–996, 1988.

Deptá, P. N., Dosta, M., Wenzel, W., Kozłowska, M., and Heinrich, S. Hierarchical coarse-grained strategy for macromolecular self-assembly: Application to hepatitis b virus-like particles. *International Journal of Molecular Sciences*, 23(23), 2022. ISSN 1422-0067. doi: 10.3390/ijms232314699. URL <https://www.mdpi.com/1422-0067/23/23/14699>.

Devlin, J., Chang, M.-W., Lee, K., and Toutanova, K. BERT: Pre-training of deep bidirectional transformers for language understanding. In *Proceedings of the 2019 Conference of the North American Chapter of the Association for Computational Linguistics: Human Language Technologies, Volume 1 (Long and Short Papers)*, pp. 4171–4186, Minneapolis, Minnesota, June 2019. Association for Computational Linguistics. doi: 10.18653/v1/N19-1423. URL <https://aclanthology.org/N19-1423>.

Donnat, C., Zitnik, M., Hallac, D., and Leskovec, J. Learning structural node embeddings via diffusion wavelets. In *Proceedings of the 24th ACM SIGKDD International Conference on Knowledge Discovery & Data Mining*, KDD ’18, pp. 1320–1329, New York, NY, USA, 2018. Association for Computing Machinery. ISBN 9781450355520. doi: 10.1145/3219819.3220025. URL <https://doi.org/10.1145/3219819.3220025>.

Dosovitskiy, A., Beyer, L., Kolesnikov, A., Weissenborn, D., Zhai, X., Unterthiner, T., Dehghani, M., Minderer, M., Heigold, G., Gelly, S., Uszkoreit, J., and Houlsby, N. An image is worth 16x16 words: Transformers for image recognition at scale. In *International Conference*

on Learning Representations, 2021. URL <https://openreview.net/forum?id=YicbFdNTTy>.

Dwivedi, V. P. and Bresson, X. A generalization of transformer networks to graphs. *CoRR*, abs/2012.09699, 2020a. URL <https://arxiv.org/abs/2012.09699>.

Dwivedi, V. P. and Bresson, X. A generalization of transformer networks to graphs. *CoRR*, abs/2012.09699, 2020b. URL <https://arxiv.org/abs/2012.09699>.

Dwivedi, V. P., Joshi, C. K., Laurent, T., Bengio, Y., and Bresson, X. Benchmarking graph neural networks. *CoRR*, abs/2003.00982, 2020. URL <https://arxiv.org/abs/2003.00982>.

Dwivedi, V. P., Luu, A. T., Laurent, T., Bengio, Y., and Bresson, X. Graph neural networks with learnable structural and positional representations. In *International Conference on Learning Representations*, 2022a. URL <https://openreview.net/forum?id=wTTjnvGphYj>.

Dwivedi, V. P., Rampasek, L., Galkin, M., Parviz, A., Wolf, G., Luu, A. T., and Beaini, D. Long range graph benchmark. In *Thirty-sixth Conference on Neural Information Processing Systems Datasets and Benchmarks Track*, 2022b. URL <https://openreview.net/forum?id=in7XC5RcjEn>.

Fang, Y., Yang, H., Zhuang, X., Shao, X., Fan, X., and Chen, H. Knowledge-aware contrastive molecular graph learning. *CoRR*, abs/2103.13047, 2021. URL <https://arxiv.org/abs/2103.13047>.

Gaul, C. and Cuesta-Lopez, S. Machine learning for screening large organic molecules. *arXiv preprint arXiv:2211.15415*, 2022.

Gilmer, J., Schoenholz, S. S., Riley, P. F., Vinyals, O., and Dahl, G. E. Neural message passing for quantum chemistry. In *Proceedings of the 34th International Conference on Machine Learning - Volume 70*, ICML'17, pp. 1263–1272. JMLR.org, 2017a.

Gilmer, J., Schoenholz, S. S., Riley, P. F., Vinyals, O., and Dahl, G. E. Neural message passing for quantum chemistry. In Precup, D. and Teh, Y. W. (eds.), *Proceedings of the 34th International Conference on Machine Learning*, volume 70 of *Proceedings of Machine Learning Research*, pp. 1263–1272. PMLR, 06–11 Aug 2017b. URL <https://proceedings.mlr.press/v70/gilmer17a.html>.

Haar, A. Zur theorie der orthogonalen funktionensysteme. *Mathematische Annalen*, 69:331–371, 1910.

Hammond, D. K., Vanderghenst, P., and Gribonval, R. Wavelets on graphs via spectral graph theory. *Applied and Computational Harmonic Analysis*, 30(2):129–150, 2011. ISSN 1063-5203. doi: <https://doi.org/10.1016/j.acha.2010.04.005>. URL <https://www.sciencedirect.com/science/article/pii/S1063520310000552>.

Hohenberg, P. and Kohn, W. Inhomogeneous electron gas. *Phys. Rev.*, 136:B864–B871, Nov 1964. doi: [10.1103/PhysRev.136.B864](https://doi.org/10.1103/PhysRev.136.B864). URL <https://link.aps.org/doi/10.1103/PhysRev.136.B864>.

Hu, W., Liu, B., Gomes, J., Zitnik, M., Liang, P., Pande, V., and Leskovec, J. Strategies for pre-training graph neural networks. In *International Conference on Learning Representations*, 2020. URL <https://openreview.net/forum?id=HJ1WWJSFDH>.

Hu, W., Fey, M., Ren, H., Nakata, M., Dong, Y., and Leskovec, J. Ogb-lsc: A large-scale challenge for machine learning on graphs. *arXiv preprint arXiv:2103.09430*, 2021.

Hy, T. S., Trivedi, S., Pan, H., Anderson, B. M., , and Kondor, R. Predicting molecular properties with covariant compositional networks. *The Journal of Chemical Physics*, 148, 2018.

Ioffe, S. and Szegedy, C. Batch normalization: Accelerating deep network training by reducing internal covariate shift. *CoRR*, abs/1502.03167, 2015. URL <http://arxiv.org/abs/1502.03167>.

Jerry, M. Advanced organic chemistry: reactions, mechanisms and structure, 1992.

Jin, W., Barzilay, R., and Jaakkola, T. Hierarchical generation of molecular graphs using structural motifs. In *Proceedings of the 37th International Conference on Machine Learning*, ICML'20. JMLR.org, 2020.

Kim, J., Nguyen, D. T., Min, S., Cho, S., Lee, M., Lee, H., and Hong, S. Pure transformers are powerful graph learners. In Oh, A. H., Agarwal, A., Belgrave, D., and Cho, K. (eds.), *Advances in Neural Information Processing Systems*, 2022. URL https://openreview.net/forum?id=um2BxfgkT2_.

Kipf, T. N. and Welling, M. Semi-supervised classification with graph convolutional networks. *arXiv preprint arXiv:1609.02907*, 2016.

Kondor, R., Hy, T. S., Pan, H., Trivedi, S., and Anderson, B. M. Covariant compositional networks for learning graphs. *Proc. ICLR Workshop*, 2018. URL <https://openreview.net/forum?id=S1TgE7WR->.

Kreuzer, D., Beaini, D., Hamilton, W., Létourneau, V., and Tossou, P. Rethinking graph transformers with spectral attention. *Advances in Neural Information Processing Systems*, 34:21618–21629, 2021.

Li, G., Xiong, C., Thabet, A. K., and Ghanem, B. Deep-ergcn: All you need to train deeper gcns. *CoRR*, abs/2006.07739, 2020a. URL <https://arxiv.org/abs/2006.07739>.

Li, P., Wang, Y., Wang, H., and Leskovec, J. Distance encoding: Design provably more powerful neural networks for graph representation learning. In *Proceedings of the 34th International Conference on Neural Information Processing Systems*, NIPS’20, Red Hook, NY, USA, 2020b. Curran Associates Inc. ISBN 9781713829546.

Li, Q., Han, Z., and Wu, X.-M. Deeper insights into graph convolutional networks for semi-supervised learning. In *Proceedings of the Thirty-Second AAAI Conference on Artificial Intelligence and Thirtieth Innovative Applications of Artificial Intelligence Conference and Eighth AAAI Symposium on Educational Advances in Artificial Intelligence*, AAAI’18/IAAI’18/EAAI’18. AAAI Press, 2018. ISBN 978-1-57735-800-8.

Liu, Z., Lin, Y., Cao, Y., Hu, H., Wei, Y., Zhang, Z., Lin, S., and Guo, B. Swin transformer: Hierarchical vision transformer using shifted windows. In *Proceedings of the IEEE/CVF International Conference on Computer Vision (ICCV)*, 2021.

Mallat, S. A theory for multiresolution signal decomposition: the wavelet representation. *IEEE Transactions on Pattern Analysis and Machine Intelligence*, 11(7):674–693, 1989. doi: 10.1109/34.192463.

Mallat, S. *A Wavelet Tour of Signal Processing, Third Edition: The Sparse Way*. Academic Press, Inc., USA, 3rd edition, 2008. ISBN 0123743702.

Maron, H., Ben-Hamu, H., Shamir, N., and Lipman, Y. Invariant and equivariant graph networks. In *International Conference on Learning Representations*, 2019. URL <https://openreview.net/forum?id=Syx72jC9tm>.

Maziarz, K., Jackson-Flux, H. R., Cameron, P., Sirockin, F., Schneider, N., Stiefl, N., Segler, M., and Brockschmidt, M. Learning to extend molecular scaffolds with structural motifs. In *International Conference on Learning Representations*, 2022. URL <https://openreview.net/forum?id=ZTsoE8G3GG>.

Morris, C., Ritzert, M., Fey, M., Hamilton, W. L., Lenssen, J. E., Rattan, G., and Grohe, M. Weisfeiler and leman go neural: Higher-order graph neural networks. In *Proceedings of the Thirty-Third AAAI Conference on Artificial Intelligence and Thirty-First Innovative Applications of Artificial Intelligence Conference and Ninth AAAI Symposium on Educational Advances in Artificial Intelligence*, AAAI’19/IAAI’19/EAAI’19. AAAI Press, 2019. ISBN 978-1-57735-809-1. doi: 10.1609/aaai.v33i01.33014602. URL <https://doi.org/10.1609/aaai.v33i01.33014602>.

Oono, K. and Suzuki, T. Graph neural networks exponentially lose expressive power for node classification. In *International Conference on Learning Representations*, 2020. URL <https://openreview.net/forum?id=S11dO2EFPr>.

Ramakrishnan, R., Dral, P., Rupp, M., and von Lilienfeld, A. Quantum chemistry structures and properties of 134 kilo molecules. *Scientific Data*, 1, 08 2014. doi: 10.1038/sdata.2014.22.

Rampášek, L., Galkin, M., Dwivedi, V. P., Luu, A. T., Wolf, G., and Beaini, D. Recipe for a General, Powerful, Scalable Graph Transformer. *arXiv:2205.12454*, 2022.

Rong, Y., Bian, Y., Xu, T., Xie, W., Wei, Y., Huang, W., and Huang, J. Self-supervised graph transformer on large-scale molecular data. In *Proceedings of the 34th International Conference on Neural Information Processing Systems*, NIPS’20, Red Hook, NY, USA, 2020. Curran Associates Inc. ISBN 9781713829546.

Ruddigkeit, L., Deursen, R., Blum, L., and Reymond, J.-L. Enumeration of 166 billion organic small molecules in the chemical universe database gdb-17. *Journal of chemical information and modeling*, 52, 10 2012. doi: 10.1021/ci300415d.

Rustamov, R. M. and Guibas, L. Wavelets on graphs via deep learning. In *Proceedings of the 26th International Conference on Neural Information Processing Systems - Volume 1*, NIPS’13, pp. 998–1006, Red Hook, NY, USA, 2013. Curran Associates Inc.

Schmid, F. Understanding and modeling polymers: The challenge of multiple scales. *ACS Polymers Au*, 0(0):null, 2022. doi: 10.1021/acspolymersau.2c00049. URL <https://doi.org/10.1021/acspolymersau.2c00049>.

Singh, S., Chaudhary, K., Dhanda, S. K., Bhalla, S., Usmani, S. S., Gautam, A., Tuknait, A., Agrawal, P., Mathur, D., and Raghava, G. P. Satpdb: a database of structurally annotated therapeutic peptides. *Nucleic acids research*, 44(D1):D1119–D1126, 2016.

Srivastava, N., Hinton, G., Krizhevsky, A., Sutskever, I., and Salakhutdinov, R. Dropout: A simple way to prevent neural networks from overfitting. *Journal of Machine Learning Research*, 15(56):1929–1958, 2014. URL <http://jmlr.org/papers/v15/srivastava14a.html>.

St. John, P. C., Phillips, C., Kemper, T. W., Wilson, A. N., Guan, Y., Crowley, M. F., Nimlos, M. R., and Larsen, R. E. Message-passing neural networks for high-throughput polymer screening. *The Journal of chemical physics*, 150(23):234111, 2019.

Sterling, T. and Irwin, J. Zinc 15 - ligand discovery for everyone. *Journal of chemical information and modeling*, 55, 10 2015. doi: 10.1021/acs.jcim.5b00559.

van der Maaten, L. and Hinton, G. Visualizing data using t-sne. *Journal of Machine Learning Research*, 9(86):2579–2605, 2008. URL <http://jmlr.org/papers/v9/vandermaaten08a.html>.

Vaswani, A., Shazeer, N., Parmar, N., Uszkoreit, J., Jones, L., Gomez, A. N., Kaiser, L., and Polosukhin, I. Attention is all you need. In *Proceedings of the 31st International Conference on Neural Information Processing Systems*, NIPS’17, pp. 6000–6010, Red Hook, NY, USA, 2017. Curran Associates Inc. ISBN 9781510860964.

Veličković, P., Cucurull, G., Casanova, A., Romero, A., Liò, P., and Bengio, Y. Graph Attention Networks. *International Conference on Learning Representations*, 2018. URL <https://openreview.net/forum?id=rJXMpikCZ>.

Wang, H., Yin, H., Zhang, M., and Li, P. Equivariant and stable positional encoding for more powerful graph neural networks. In *International Conference on Learning Representations*, 2022. URL <https://openreview.net/forum?id=e95i1IHcWj>.

Xu, B., Shen, H., Cao, Q., Qiu, Y., and Cheng, X. Graph wavelet neural network. In *International Conference on Learning Representations*, 2019a. URL <https://openreview.net/forum?id=H1ewdiR5tQ>.

Xu, B., Shen, H., Cao, Q., Qiu, Y., and Cheng, X. Graph wavelet neural network. In *International Conference on Learning Representations*, 2019b. URL <https://openreview.net/forum?id=H1ewdiR5tQ>.

Xu, K., Hu, W., Leskovec, J., and Jegelka, S. How powerful are graph neural networks? In *7th International Conference on Learning Representations, ICLR 2019, New Orleans, LA, USA, May 6-9, 2019*. OpenReview.net, 2019c. URL <https://openreview.net/forum?id=ryGs6iA5Km>.

Yang, M., Shen, Y., Li, R., Qi, H., Zhang, Q., and Yin, B. A new perspective on the effects of spectrum in graph neural networks. In Chaudhuri, K., Jegelka, S., Song, L., Szepesvari, C., Niu, G., and Sabato, S. (eds.), *Proceedings of the 39th International Conference on Machine Learning*, volume 162 of *Proceedings of Machine Learning Research*, pp. 25261–25279. PMLR, 17–23 Jul 2022. URL <https://proceedings.mlr.press/v162/yang22n.html>.

Ying, C., Cai, T., Luo, S., Zheng, S., Ke, G., He, D., Shen, Y., and Liu, T.-Y. Do transformers really perform badly for graph representation? In Beygelzimer, A., Dauphin, Y., Liang, P., and Vaughan, J. W. (eds.), *Advances in Neural Information Processing Systems*, 2021. URL <https://openreview.net/forum?id=OeWooOxFwDa>.

Ying, R., You, J., Morris, C., Ren, X., Hamilton, W. L., and Leskovec, J. Hierarchical graph representation learning with differentiable pooling. In *Proceedings of the 32nd International Conference on Neural Information Processing Systems*, NIPS’18, pp. 4805–4815, Red Hook, NY, USA, 2018. Curran Associates Inc.

You, J., Ying, R., and Leskovec, J. Position-aware graph neural networks. In Chaudhuri, K. and Salakhutdinov, R. (eds.), *Proceedings of the 36th International Conference on Machine Learning*, volume 97 of *Proceedings of Machine Learning Research*, pp. 7134–7143. PMLR, 09–15 Jun 2019. URL <https://proceedings.mlr.press/v97/you19b.html>.

Yun, S., Jeong, M., Kim, R., Kang, J., and Kim, H. J. Graph transformer networks. In Wallach, H., Larochelle, H., Beygelzimer, A., d’Alché-Buc, F., Fox, E., and Garnett, R. (eds.), *Advances in Neural Information Processing Systems*, volume 32. Curran Associates, Inc., 2019. URL <https://proceedings.neurips.cc/paper/2019/file/9d63484abb477c97640154d40595a3bb-Paper.pdf>.

A. Implementation Details

A.1. Multiresolution Graph Transformer

Table 3. The hyperparameters for MGT

Hyperparameters	Values
No. Epoch	200
Embedding Dimension	84
Batch size	128
Learning rate	0.001
Dropout	0.25
Attention Dropout	0.5
Diffusion Step (K)	[1, 2, 3, 4, 5]
No. Head	4
Activation	ReLU
Normalization	Batchnorm
No. Cluster	10
λ_1	0.001
λ_2	0.001

In this section, we elaborate on the architecture and hyperparameters used to train and evaluate our MGT to achieve the above numerical results. Table 3 show details of the hyperparameters used for MGT in all the experiments. In particular, we use the atom and bond encoder modules provided by OGB (Hu et al., 2021) to attribute the molecular graph. We use two GPS layers to compute the atom-level representations and two Transformer layers for calculating the substructure-level representations. For learning to cluster, we use a 2-layer message-passing network to compute \mathbf{Z} and \mathbf{S} mentioned in Eq. (5) (6) as follows:

$$\mathbf{Z}_a^1, \mathbf{E}_a^1 = \text{GatedGCN}^1(\mathbf{X}_a, \mathbf{E}_a, \mathbf{A}) \quad (14)$$

$$\mathbf{Z}_a^1 = \text{Batchnorm}(\text{ReLU}(\mathbf{Z}_a^1)) \quad (15)$$

$$\mathbf{Z}_a^2, \mathbf{E}_a^2 = \text{GatedGCN}^2(\mathbf{Z}_a^1, \mathbf{E}_a^1, \mathbf{A}) \quad (16)$$

$$\mathbf{Z}_a^2 = \text{Batchnorm}(\text{ReLU}(\mathbf{Z}_a^2)) \quad (17)$$

$$\mathbf{Z} = \text{concat}(\mathbf{Z}_a^1, \mathbf{Z}_a^2) \quad (18)$$

$$\mathbf{Z} = \text{FFN}(\mathbf{Z}) \quad (19)$$

\mathbf{S} is computed similarly with an auxiliary Softmax operation on the output to produce a probabilistic clustering matrix.

A.2. Baselines used in Polymer Property Prediction

Table 4 shows the implementation of the baselines we used in the polymer experiments. All the models are designed to have approximately 500 to 700k learnable parameters. For fair comparisons, all the models are trained in 50 epochs with a learning rate of 0.001 and batch size of 128.

Table 4. The detailed settings of baselines for polymer property prediction

Model	No. Layer	Embed Dim	No. Params
GCN + Virtual Node	5	156	557k
GINE + Virtual Node	5	120	557k
GPS	3	120	600k
Transformer + LapPE	6	120	700k

B. Visualization

We use the t-SNE algorithm (van der Maaten & Hinton, 2008) to project the representations produced by MGT (with WavePE) of peptides and polymers of the test datasets into two-dimensional spaces for visualization. Also, we take the probabilistic clustering matrix \mathbf{S} in Eq. (6) to visualize the clustering results on the molecules. Specifically, we use the RDKit package³ to draw the molecules.

B.1. Representations of Peptides

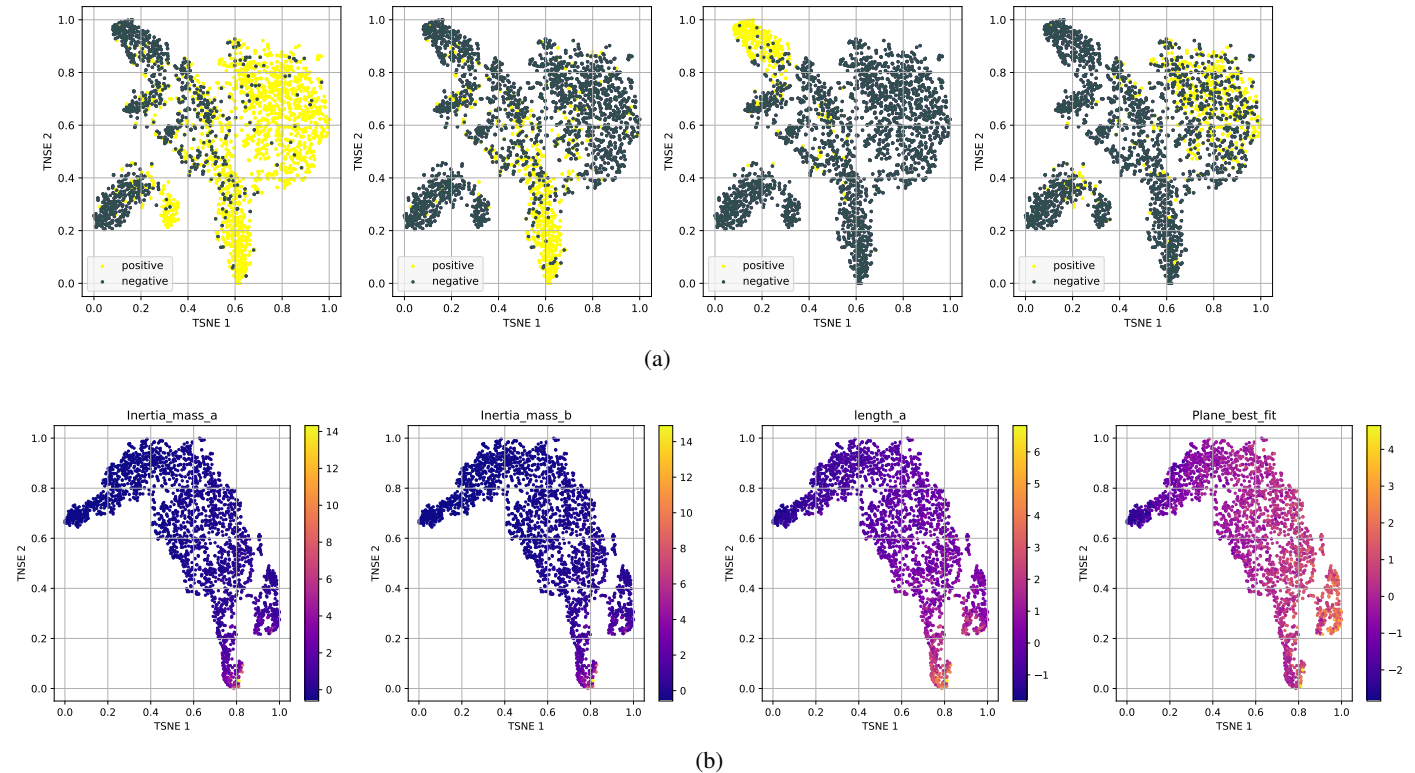


Figure 4. Visualization of low-dimensional spaces of peptides on two property prediction tasks: Peptides-func and Peptides-struct. All the vectors are normalized to range $[0, 1]$. a) t-SNE projection of peptides taken from the Peptides-func testing dataset. We take four random peptide functions, and each figure corresponds to one of the properties with positive (1) and negative (0) ground truths. b) Similarly, we plot the figures of four random peptide properties taken from the Peptides-struct testing dataset. The spectrums represent continuous ground truths, where lower values correspond to cooler colors.

³RDKit: Open-source cheminformatics. <https://www.rdkit.org>

B.2. Representations of Polymers

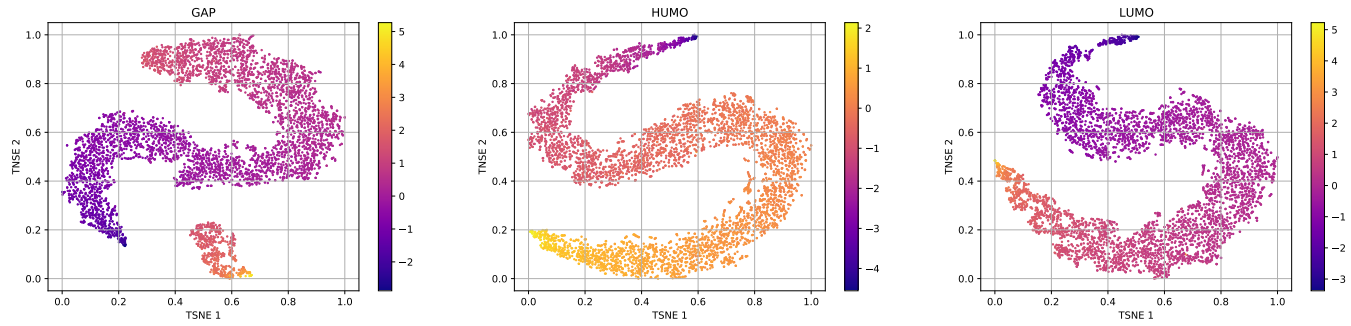


Figure 5. t-SNE projection of representations of the test polymers in the dataset. We plot the figures of three properties, including GAP, HUMO, and LUMO. As the labels are continuous values, points are color-coded by spectrums wherein higher values correspond to warmer palettes.

B.3. Clustering on Peptides

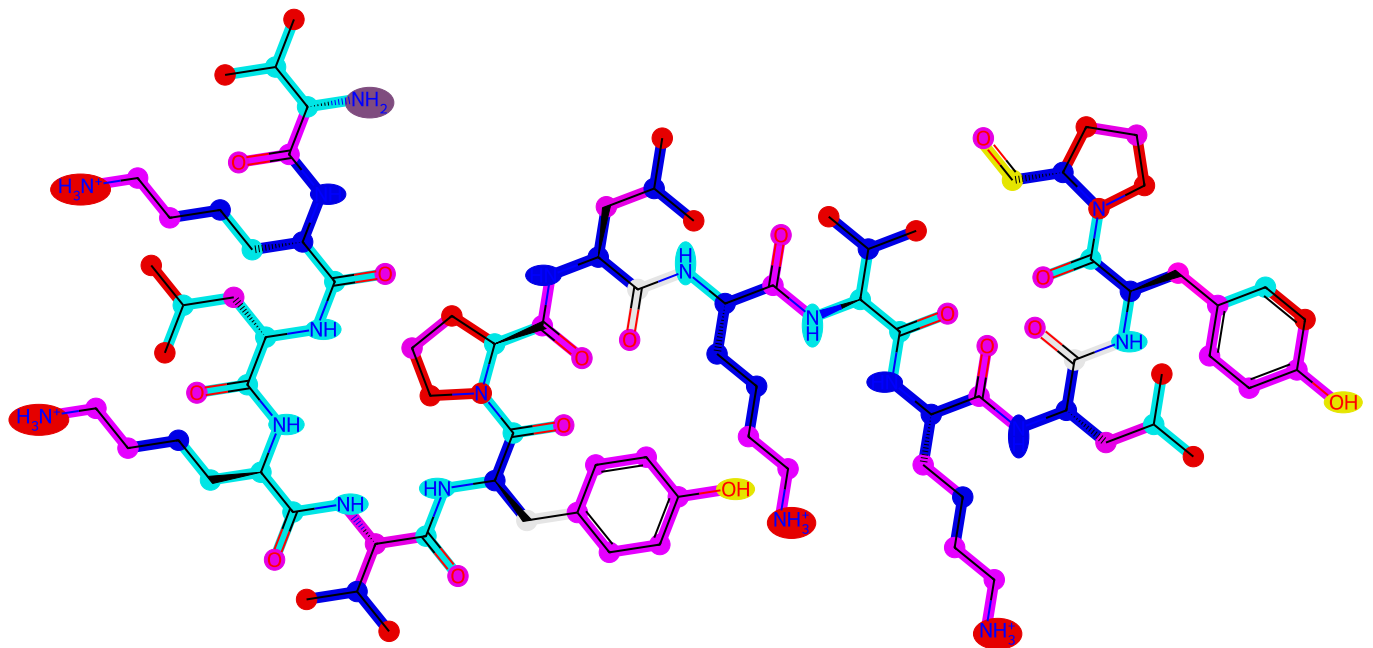


Figure 6. The clustering result on a peptide. MGT can group the atoms of a long peptide into different substructure types. Specifically, the groups NH3 and OH are recognized even though the atoms are located distantly. Also, local rings or segments are also detected.

B.4. Clustering on Polymers

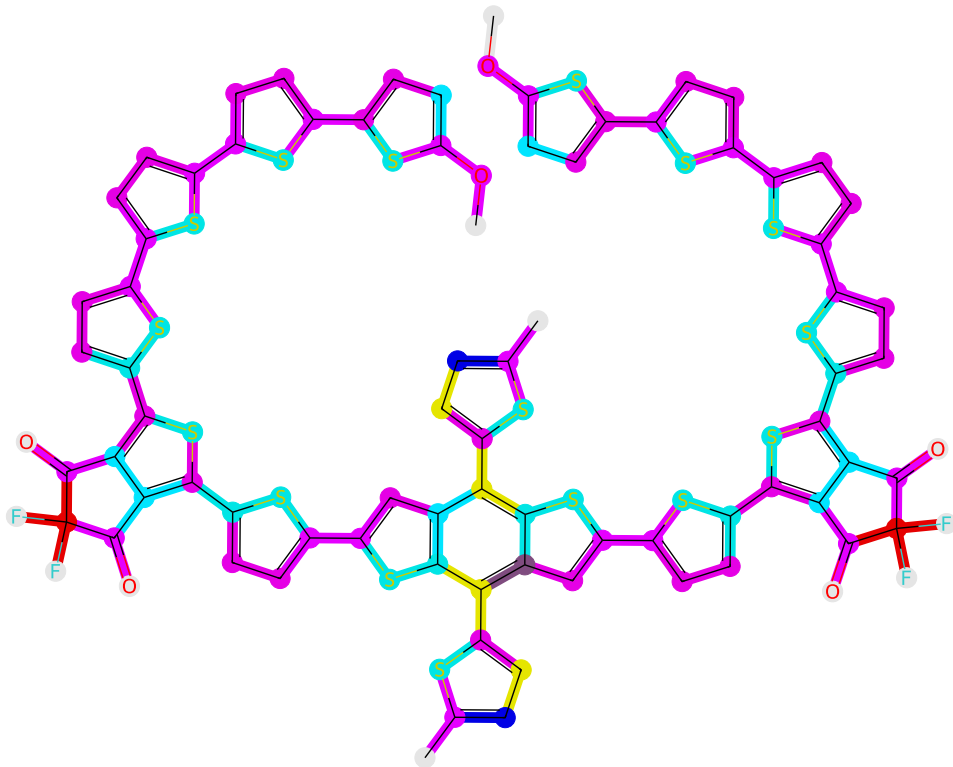


Figure 7. The clustering result on a polymer. By learning to cluster and using a substructure-level Transformer encoder, MGT can model repetitive patterns existing in polymers. In this example, the model can recognize repeating units in a long-chain polymer or even symmetries.

C. Experiments on Small Molecules

Although MGT is intentionally designed for learning to represent hierarchical structures, we report its experimental results on the ZINC-12K dataset (Sterling & Irwin, 2015), which consists of small drug-like molecules, in this section. We train MGT to predict the solubility (LogP) of the molecules with up to 50 heavy atoms on a subset of the ZINC dataset. We follow the split of 10K/1K/1K for training/validation/testing proposed in (Dwivedi et al., 2020). Baseline results include GCN (Kipf & Welling, 2016), GINE (Xu et al., 2019c; Dwivedi et al., 2020), , GAT (Veličković et al., 2018), Spec-GN (Yang et al., 2022), PNA (Corso et al., 2020a), GatedGCN (Bresson & Laurent, 2017), GPS (Rampášek et al., 2022), MPNN (Gilmer et al., 2017a), SAN (Kreuzer et al., 2021), DGN (Li et al., 2020a), and Graphomer (Ying et al., 2021). Our MGT + WavePE outperforms 7 out of 10 other baselines.

Table 5. Experimental results on the ZINC-12K dataset

Method	No. Params	MAE \downarrow
GCN	505k	0.367 ± 0.011
GINE	510k	0.526 ± 0.051
GAT	531k	0.384 ± 0.007
PNA	387k	0.142 ± 0.010
MPNN	418k	0.145 ± 0.007
GatedGCN	505k	0.214 ± 0.006
SAN	509k	0.139 ± 0.006
Graphomer	489k	0.122 ± 0.006
GPS	-	0.070 ± 0.004
Spec-GN	503k	0.0698 ± 0.002
MGT + WavePE (ours)	499k	0.131 ± 0.003